Adsorption 4, 361–372 (1998)

Application of Surface Diffusion Model to the Adsorption of Dyes on Bagasse Pith

GORDON MCKAY
Department of Chemical Engineering, The Hong Kong University of Science and Technology, Clear Water Bay, Kowloon, Hong Kong

Abstract. A homogeneous solid phase diffusion model (HSDM) has been developed using a computer to predict the performance of a batch adsorber. The computer program utilises a semi-analytical solution for a two resistance model based on external mass transfer and homogeneous solid phase diffusion. The model has been successfully applied to four adsorption systems, namely, the adsorption of AB25, AR114, BB69 and BR22 onto pith. The method produces excellent correlations between experimental and theoretical concentration decay curves in batch adsorbers. The model developed presents a solution using a single solid diffusion coefficient and a single external mass transfer coefficient which are sufficient to characterise the system within a range of initial dye concentration, 25–300 mg . dm^3 and solid/liquid ratios (w/v) 0.25–2.

Keywords: dyestuffs, modeling, HSDM, equilibrium, film diffusion

Introduction

An effective adsorption model requires an accurate equilibrium isotherm, kinetic/mass transfer relationships and coupling equations. The mass transfer stage usually assumes a three-step model: (i) external film diffusion across the boundary layer, (ii) adsorption at a surface site, and (iii) internal mass transfer within the particle based on a pore diffusion or solid surface diffusion mechanism.

Various assumptions have been applied to equilibrium data, linear isotherm (Dryden and Kay, 1954), irreversible isotherm (Liapis and Rippin, 1977, 1978; McKay, 1984) and nonlinear isotherm (Tien, 1960, 1961; Weber and Rummer, 1965). Specific cases of nonlinear isotherms include, Langmuir equation (Langmuir, 1918; Spahn and Schlunder, 1975; McKay, 1982; McKay and Al Duri, 1990), Freundlich equation (Freundlich, 1913; El-Dib et al., 1978; McKay et al., 1980; Moon and Lee, 1983; McKay and Al Duri, 1988; Glover et al., 1990; Young et al., 1991), Redlich-Peterson equation (Redlich and Peterson, 1959; Mathews and Weber, 1976; Jossens et al., 1978; Seidel et al., 1986; McKay and Al Duri, 1989). A full description of isotherm classifications and applications has been presented in a review by Al Duri (1995).

The homogeneous solid diffusion model (HSDM) has probably received more attention than other mechanisms for predicting internal adsorptive mass transfer. The model has been used by Millar and Clump (1970), Hashimoto et al. (1975), Rice (1982), Crittenden and Weber (1978a, 1978b) and Crittenden et al. (1985).

The film-solid diffusion model has also been extended to multicomponent systems by Mathews (1975). Numerical solution of Crank-Nicolson's finite difference method yielded the rate equation. Crittenden (1976) adopted the same approach with the fixed bed adsorption of binary systems. Thomas and Lombardi (1971) have used it to describe experimental breakthrough curves for the adsorption of vapour mixtures from an inert gas onto carbon. Liapis and Rippin (1977) solved the film-solid diffusion for batch reactors by orthogonal collocation. The resulting equations were solved by an iterative scheme that involved numerical integration of the rate equation and solution of nonlinear algebraic equations for conditions. Mathews (1975), Crittenden (1976), Liapis and Rippin (1977) and Fritz et al. (1981) have all assumed constant

diffusivities (D_s, cm^2 s^{-1}) independent of concentration and time for a given set of conditions. Neretnieks (1976) studied D_s as a function of the sorbent surface coverage. Generally, the film-solid diffusion model gave accurate results for multicomponent systems with similar diffusional behaviour. With systems of vast difference in diffusive properties, systematic deviations were encountered. Nonetheless, due to its adequacy in describing the widest range of single and multicomponent systems, the film-solid diffusion model was selected for further research in the field (Mathews, 1975; Smith et al., 1987; Thacker et al., 1984). The present paper applies a semi-analytical solution to the HSDM to predict the adsorption of four dyestuffs onto bagasse pith, a waste product from the sugar cane industry.

Theory

Adsorption rate data from batch reactors have been analysed using a model that includes the effects of external mass transfer, unsteady state intraparticle diffusion in the particle and a nonlinear adsorption isotherm. The theoretical model is based on the fundamental assumptions proposed by Mathews and Weber (1976) in which the adsorbent particles are assumed to be identical spheres of radius R.

Fundamental Equations

External mass transfer resistance in a completely mixed adsorber is principally in the hydrodynamic film surrounding the particle. Mass transfer from the fluid phase to the solid surface is expressed in terms of the time rate of the average solute concentration, $\bar{q}_t$, of the particle,

$$\frac{d\bar{q}_t}{dt} = \frac{k_f \cdot A_p}{V_p \cdot \rho_p}(C_t - C_s) \tag{1}$$

The average solute concentration of the particle is obtained by integrating the pointwise concentration over the volume of the particle.

$$\bar{q}_t = \frac{3}{R^3}\int_0^R q \cdot r^2 \cdot dr \tag{2}$$

The isotherm expression may be written in the general form of the three parameter Redlich-Peterson isotherm (1959):

$$q_s = (K_R \cdot C_s)\big/\left(1 + a_R \cdot C_s^{\beta}\right) \tag{3}$$

where $\beta \leq 1.0$.

Transport within the solid phase for a spherical particle, assuming symmetry in two directions, is given by

$$\frac{\partial q}{\partial t} = D_s\left[\frac{\partial^2 q}{\partial r^2} + \frac{2}{r}\cdot\frac{\partial q}{\partial r}\right] \tag{4}$$

The material balance equation for a slurry adsorber is

$$V \cdot \frac{dC_t}{dt} = -W \cdot \frac{d\bar{q}_t}{dt} \tag{5}$$

The initial and boundary conditions for the fluid and solid phases are given as

$$C_t(0) = C_0 \tag{6}$$

$$\bar{q}_t(r, 0) = 0 \tag{7}$$

$$q(R, t) = q_s(t) \tag{8}$$

$$\frac{\partial q}{\partial t}(0, t) = 0 \tag{9}$$

The initial concentration of solute in the liquid phase is C_0, and zero in the solid phase. The surface concentration in the solid phase is an unknown function of time, and the flux at the centre of the particle is zero at all times.

The independent variables in Eq. (4) can be transformed into dimensionless variables:

$$\tau = (D_s \cdot t)/R^2 \quad \text{and} \quad z = r/R \tag{10}$$

Subsequent change of variable with $u = z \cdot q$ and rearrangement gives the following set of equations for adsorption in a batch reactor.

$$\frac{\partial u}{\partial \tau} = \frac{\partial^2 u}{\partial z^2} \tag{11}$$

$$u(0, \tau) = 0 = u(z, 0) \tag{12}$$

$$u(1, \tau) = u_s(\tau) \tag{13}$$

$$\int_0^1 \frac{\partial u}{\partial \tau}\cdot z \cdot d_z = \frac{3k_f \cdot R(C_t - C_s)}{D_s \cdot \rho_p(1-\varepsilon)} \tag{14}$$

$$\bar{q}_t = 3\int_0^1 u \cdot z \cdot d_z \tag{15}$$

$$V \cdot \frac{dC_t}{dt} = -W \cdot \frac{d\bar{q}_t}{dt} \tag{16}$$

Method of Solution

These Eqs. (11)–(16) and (3) are difficult to solve analytically, and a finite difference technique was employed by Mathews and Weber (1976). These equations were solved using the implicit finite difference scheme of Crank-Nicholson.

McKay et al. (1984) have proposed a semi-analytical integral formulation solution of the diffusion Eq. (11). The starting point is a semi-analytical solution of the diffusion equation which satisfies the boundary conditions:

$$u(z,\tau)=\int_0^{\tau} d\tau' f(\tau')\frac{1}{\sqrt{(\tau-\tau')}} \times \left\{e^{-(z-1)^{0.5}(\tau-\tau')}-e^{-(z+1)^{0.5}(\tau-\tau')}\right\} \quad (17)$$

The following approximation is then derived:

$$u(z,\tau_n)\approx 3\cdot\sum_{j=1}^{n} f_i G_i(z,\tau_n) \quad (18)$$

Where f_i is the average value of $f(\tau)$ in the interval τ_{i-1} to τ_i and

$$G_i(z,\tau_n)=\int_{\tau_{i-1}}^{\tau_1} d\tau' \frac{1}{\sqrt{(\tau_n-\tau')^{1/2}}} \times \left\{e^{-(z-1)^{**2/4}(\tau_n-\tau')}-e^{-(z+1)^{**2/4}(\tau_n-\tau')}\right\} \quad (19)$$

Similar approximations are then made for q for Eq. (14) and $\partial q/\partial\tau(\partial uz\partial z/\partial\tau)$ of (14). With suitable initial values for $q(\tau_0)$ and $C(\tau_0)=C_0$ it is the possible to calculate values for these quantities at τ_1 and for q_s at τ_1. By repeating the cycle the quantities can be calculated at time τ_n.

A result $u(z,\tau)$ is a solution of Eq. (11) via Eqs. (17) to (19) and a general form of this solution is given by Eq. (20).

$$u(z,\tau)_0=\int_0^{\tau_n} d\tau f(\tau')\frac{1}{(\tau_n-\tau')^{0.5}} \times\left[\exp\left[\frac{-(z-1)^2}{4(\tau_n-\tau')}\right]-\exp\left[\frac{-(z+1)^2}{4(\tau_n-\tau')}\right]\right] \quad (20)$$

The equations developed in this section can be used analytically with the aid of a computer to obtain the kinetic concentration decay curve, given the necessary mass transfer and equilibrium parameters.

Experimental

Materials

Adsorbent-Bagasse Pith. In the manufacture of sugar, the sugar cane stalks are chopped to small pieces by rotary knives, and extracted by crushing them through one or more roller mills. During this process more than 95% of the sucrose content of the cane is removed. The waste residual material from this operation is termed bagasse pith.

The moisture content of bagasse pith was 14.5 ± 0.5%, and it was not subjected to any form of pretreatment prior to use. The pith particles were sieved in the laboratory into various particle size ranges.

The Egyptian bagasse pith was subjected to chemical analysis (Saad et al., 1978) and the results obtained are given in Table 1.

Adsorbates. The adsorbates and their structures used in the experiments are listed below. The dyestuffs were used as the commercial salts.

(1) Acid Blue 25 (Telon Blue ANL) CI 62055 was supplied by Bayer.

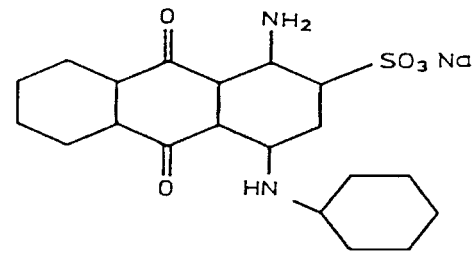

(2) Acid Red 114 (Erionyl Red RS) CI 23635 was supplied by Ciba-Geigy.

Table 1. Chemical analysis of the bagasse pith.

Determination	%
α-Cellulose	53.7
Pentosan	27.9
Lignin	20.2
Alcohol/benzene solubility	7.5
Ash	6.6

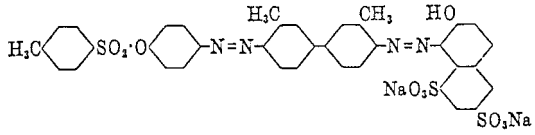

(3) Basic Red 22 (Maxilon Red BL-N) CI 11055 was supplied by Ciba-Geigy.

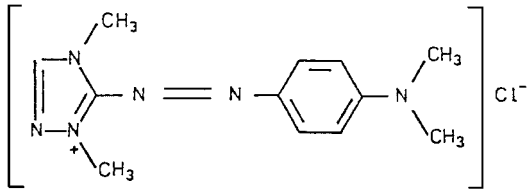

(4) Basic Blue 69 (Astrazone Blue FRR) was supplied by Bayer.

No structure is available for this dye. It belongs to the methine class, of which the chromophore is a conjugate chain of carbon atoms terminated by an ammonium group, and in addition, a nitrogen, sulphur, or oxygen atom, or an equivalent unsaturated group. A general structure for the methine class is:

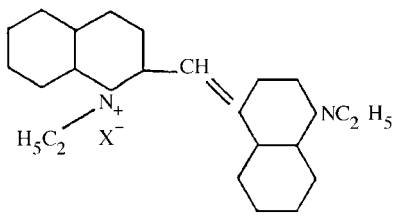

Analytical Technique

The dyes were made up in stock solutions of concentration 1000 ppm and were subsequently diluted to required concentrations. Calibration curves for each dye were prepared by recording the absorbance values for a range of known concentrations of dye solution at the wavelength for maximum absorbance of each dye. This value, λ_{max}, was found from a full scan of the dye's spectrum and the values are given in Table 2. These values of λ_{max} were used in all subsequent investigations using the four dyes. All readings were performed using a Perkin-Elmer Model 550S Spectrophotometer.

Table 2. Maximum absorbance wavelength of dyes.

Dye	Abbreviation	λ_{max} (nm)
Acid blue 25	AB25	600
Acid red 114	AR114	522
Basic blue 69	BB69	585
Basic red 22	BR22	538

Batch Experiments

Two series of batch-type experiments were carried out. Adsorption equilibrium isotherms were derived from small-scale batch experiments and kinetic data were derived from larger scale "contact time" experiments.

Equilibrium Experiments. The equilibrium isotherms were determined by contacting a constant mass of pith (0.10 g—BB69 and BR22; 0.30 g—AB25 and AR114) with 0.050 dm^3 dye solution in sealed glass bottles in a Griffin constant temperature, constant agitation shaker bath. In each isotherm run the dye solution concentration ranged from 20 to 450 ppm. Isotherms were prepared using a discrete particle size range of bagasse pith and for a range of temperature: 20°C (room temperature ±2°C), 40°C, 60°C and 80°C. An equilibrium time of five days was found to be satisfactory for each dye. After this time the samples were filtered and their equilibrium concentrations determined by spectrophotometry and reference to the calibration curves. The results were treated as follows:

$$q_e = 0.05(C_0 - C_e)/M \tag{21}$$

q_e was plotted against C_e to give the isotherm curves.

Kinetic Experiments. These experiments were used to investigate the influence of several system variables on the adsorption rate. An adsorber vessel with a standard tank configuration was used in all of the experiments.

The adsorber vessel used, was a 2 dm^3 glass beaker of internal diameter 0.13 m holding a volume of 1.7 dm^3 of dye solution. Mixing was provided by a six bladed, flat stainlesssteel impeller of 0.065 m diameter and a blade height of 0.013 m. A Heidolph Type 5011 variable speed motor was used to drive the impeller using a 0.013 m diameter stainless stell shaft. Eight anodized aluminium baffles were evenly spaced around the circumference of the vessel, positioned at 45° intervals.

Aluminium baffles were 0.2 m long and 0.01 m wide and were positioned approximately one quarter of the baffle width from the vessel wall and bottom in order to prevent particle accumulation. Evaporation of liquid was prevented by using a thick polythene sheet over the top of the adsorber vessel.

Results and Discussion

Equilibrium Studies

The equilibrium curves for the four dyes on bagasse pith are shown in Fig. 1. The mathematical solution of the homogeneous surface diffusion model used in this paper is best facilitated by an equilibrium isotherm equation containing an exponential component. The equilibrium data were analysed using the Freundlich (1913) and Redlich-Peterson (1959) isotherms. The Redlich-Peterson isotherm incorporates the features of the Langmuir (1918) and Freundlich expressions and is represented by the following expression:

$$q_e = (K_R C_e) \big/ \left(1 + a_R \cdot C_e^{\beta}\right) \qquad (22)$$

where $\beta \leq 1.0$.

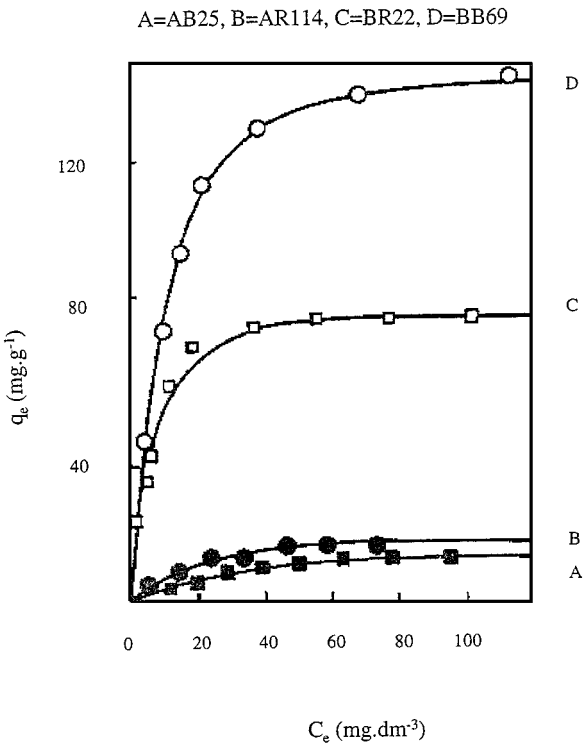

Figure 1. Equilibrium curves for the adsorption of the four dyes on bagasse pith.

The linear form is shown in Eq. (23) from which the constants, K_R, a_R and β are determined. The constant K_R is handed as a variable and the value of K_R selected is the value which optimises the data correlation coefficient for Eq. (22).

$$\log\left[\frac{K_L \cdot C_e}{q_e} - 1\right] = \log a_R + \beta \log C_e \qquad (23)$$

A Redlich-Peterson isotherm is given a more realistic representation of the system than the Freundlich equation over a wide range of conditions. Furthermore, higher correlation coefficients were obtained for the data. The results are presented in Table 3.

HSD Model

The mass transport model is based on external mass transfer and homogeneous solid phase diffusion. A program was developed to give the theoretical concentration decay curve with corresponding surface equilibrium conditions using the two resistance approach. The principal parameters required for the use of the program were the external mass transfer coefficient k_f and the solid phase diffusion coefficient D_s. Initially the value of the external mass transfer coefficient k_f was taken from a single resistance analysis value. This k_f value was obtained by a method developed for the sorption of dyes on chitin (McKay et al., 1983) for nonlinear isotherms.

By iterating between the external mass transfer coefficient k_f and the solid phase diffusion coefficient D_s, it is possible to obtain a "best fit" to the experimental decay curves for batch adsorption. This iterative method was used to obtain an "average best fit D_s" for each dye-pith system. This D_s was subsequently used to generate the theoretical concentration versus time decay curves discussed later in this paper.

The model has been applied extensively for the adsorption of AB25, AR114, BB69 and BR22 onto pith. The variables studied were:

(i) initial dye concentration;
(ii) pith mass.

The effect of initial dye concentration is shown in Figs. 2 and 3 for a wide range of initial dye concentrations for the two Acid Dyes. The correlation between experimental and theoretical results is excellent, and the fitted parameters, k_f and D_s are given in Table 4. It was found that the parameters, k_f and D_s were constant

Table 3. Redlich-Peterson constants for the various adsorption systems.

Dye	d_p (μm)	Temp. (°C)	K_R ($dm^3 \cdot g^{-1}$)	a_R ($dm^3 \cdot mg^{-1}$)	β	Correlation coefficient
BB69	250–355	20	21.6	0.157	0.95	0.99
	355–500	20	18.8	0.157	0.93	0.99
	500–710	20	15.9	0.136	0.93	0.99
	710–1000	20	11.5	0.106	0.91	0.99
	710–1000	40	14.9	0.135	0.91	0.99
	710–1000	60	19.1	0.167	0.90	0.99
	710–1000	80	24.4	0.201	0.90	0.99
BR22	500–710	20	18.0	0.313	0.93	0.99
AB25	250–355	20	0.74	0.043	0.94	0.99
	355–500	20	0.61	0.041	0.91	0.99
	500–710	20	0.50	0.036	0.88	0.98
	710–1000	20	0.36	0.020	0.95	0.99
	500–710	40	0.65	0.035	0.97	0.99
	500–710	60	0.87	0.034	0.99	0.99
	500–710	80	1.10	0.027	0.99	0.98
AR114	500–710	20	1.10	0.032	0.99	0.99

and were sufficient to fit a wide range of experimental conditions for each system.

In Fig. 2, for the adsorption of AB25 onto bagasse pith, the agreement between theoretical and experimental data at the three lower initial dye concentrations is excellent. At the three higher concentrations, after around 90 minutes, the theoretical concentration decay curve begins to decrease faster than the experimental concentrations decay points. At higher dye concentrations and at longer contact times it is not to

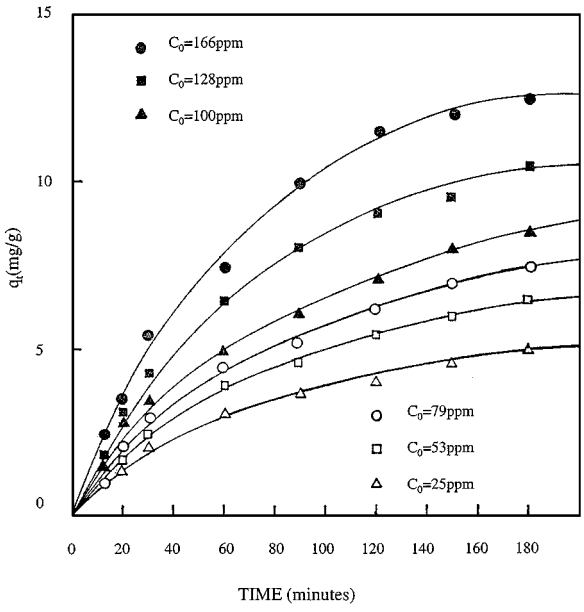

Figure 2. Effect of initial dye concentration on adsorption of AB25 onto pith.

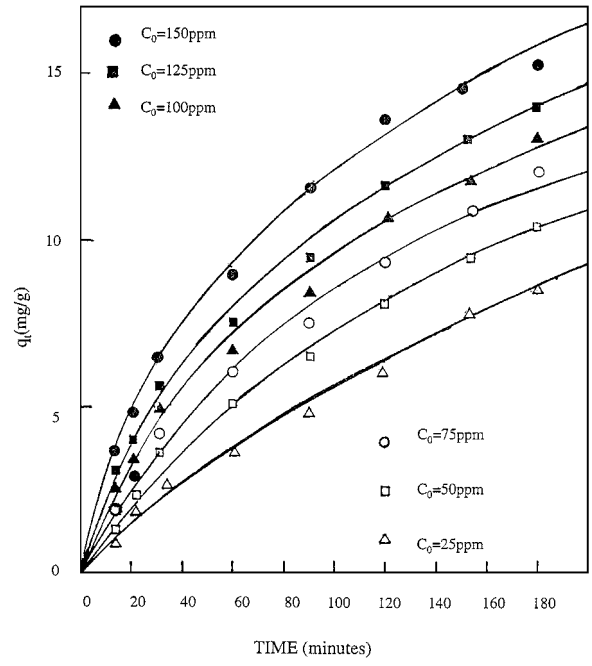

Figure 3. Effect of initial dye concentration on adsorption of AR114 onto pith.

Table 4. External mass transfer and solid-phase diffusion coefficients for the adsorption of acid dyes onto pith.

Run No.	Dye	C_o (mg · dm^{-3})	M (g)	$k_f \times 10^{-6}$ (m s^{-1})	$D_s \times 10^{-13}$ (m^2 s^{-1})
1	AB25	26	3.4	8.0	6.0
2		53	3.4	8.0	6.0
3		79	3.4	8.0	6.0
4		100	3.4	8.0	6.0
5		129	3.4	8.0	6.0
6		166	3.4	8.0	6.0
7		100	0.85	8.0	6.0
8		100	1.275	8.0	6.0
9		100	1.7	8.0	6.0
10		100	2.125	8.0	6.0
11		100	2.55	8.0	6.0
12		100	3.4	8.0	6.0
1	AR114	25	3.4	5.0	3.0
2		50	3.4	5.0	3.0
3		75	3.4	5.0	3.0
4		100	3.4	5.0	3.0
5		125	3.4	5.0	3.0
6		150	3.4	5.0	3.0
7		100	0.85	5.0	3.0
8		100	1.275	5.0	3.0
9		100	1.70	5.0	3.0
10		100	2.125	5.0	3.0
11		100	2.55	5.0	3.0
12		100	3.4	5.0	3.0

$d_p = 605 \times 10^{-4}$ cm, agitation speed = 400 rpm, $T = 20°$C, $V = 1.7$ dm^3 and $\rho_p = 0.804$ g · cm^{-3}.

be unexpected if pore diffusion from liquid filled pores within the particle starts to have an effect on the rate controlling mechanism. In Fig. 3, for the adsorption of AR114 onto pith, almost all the experimental and theoretical data correlate well.

Figures 4 and 5 show the effect of initial dye concentration on the concentration versus time decay curves for the two basic dyes. Figure 4 represents the adsorption of BB69 onto bagasse pith and shows that, for the two higher concentrations, namely $C_0 = 250$ mg · dm^{-3} and $C_0 = 300$ mg · dm^{-3}, the experimental data are decreasing more rapidly than the theoretical concentration curves. Similarly, Fig. 5, for the adsorption of BR22 on pith, shows the experimental concentration decay data points decrease more rapidly than the theoretical decay curves. Since the deviation between

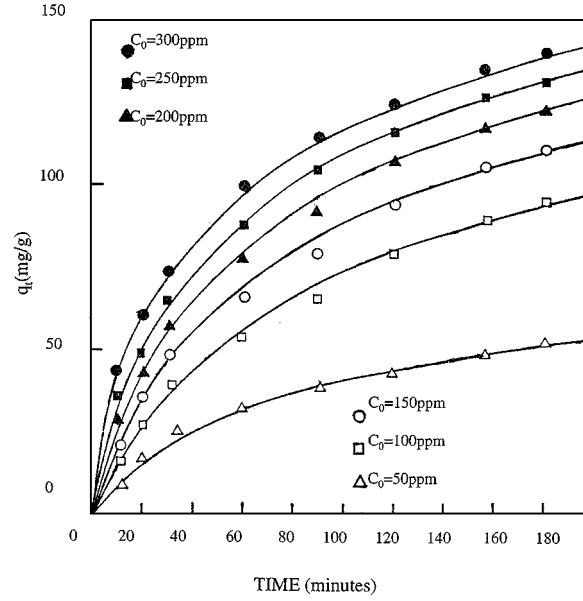

Figure 4. Effect of initial dye concentration on adsorption of BB69 onto pith.

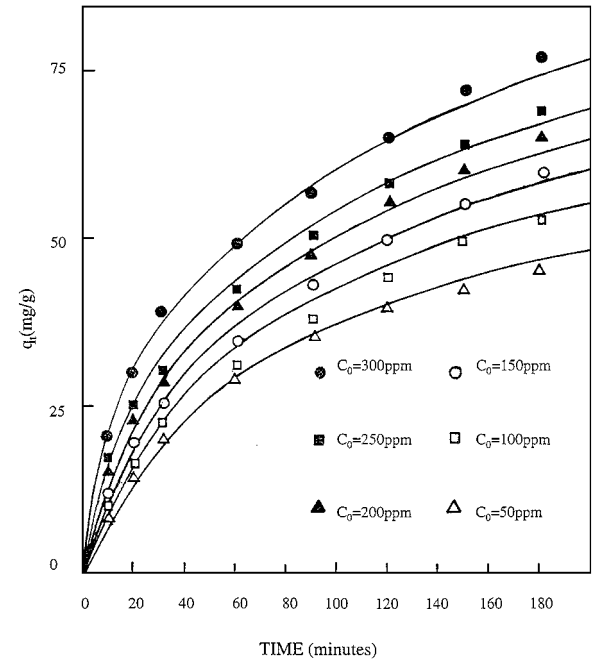

Figure 5. Effect of initial dye concentration on adsorption of BR22 onto pith.

experimental and theoretical data increase with increasing contact time and with increasing dye concentration it is almost certainly due to an increasing contribution from pore diffusion.

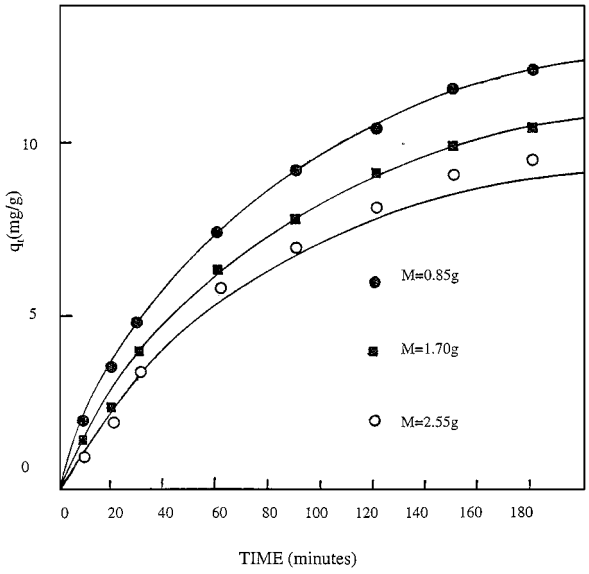

(a)

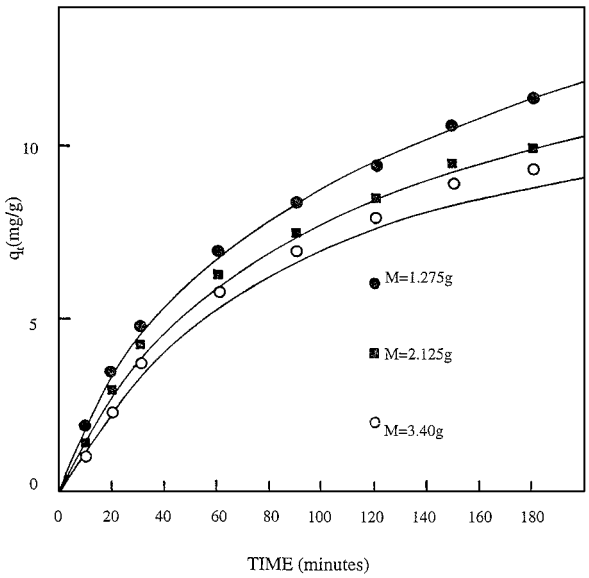

(b)

Figure 6. Effect of pith mass on the adsorption of AB25.

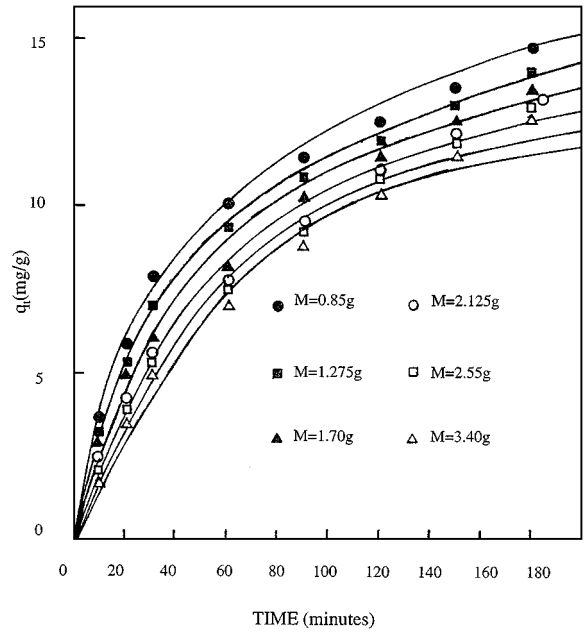

Figure 7. Effect of pith mass on the adsorption of AR114.

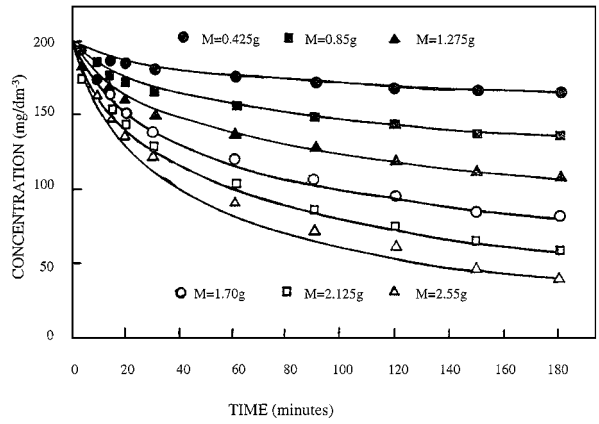

Figure 8. Effect of pith mass on the adsorption of BB69.

Figures 6 and 7 show the effect of varying the mass of bagasse pith added to a solution of initial dye concentration, $C_0 = 100$ mg · dm^{-3}, for the two acid dyes, namely AB25 and AR114. The correlation between the theoretical decay curves and the experimental data points in most cases is extremely good except for the two high adsorbent masses for both dyestuffs. The disparity could be due to some limited surface heterogeneity which is only apparent at very high solid surface area to dye mass ratios.

Figures 8 and 9 show the effect of varying the mass of bagasse pith added to a solution of initial dye concentration, $C_0 = 200$ mg · dm^{-3}, for the two basic dyes BB69 and BR22. A similar trend occurs for these two systems at high bagasse pith mass as occurred for the two acid dyes. Otherwise the correlation between experimental and theoretical data is excellent. Furthermore, even for the two high masses the disparity between the data for the two basic dye systems is not as great as for the acid dyes. This is probably because the solid

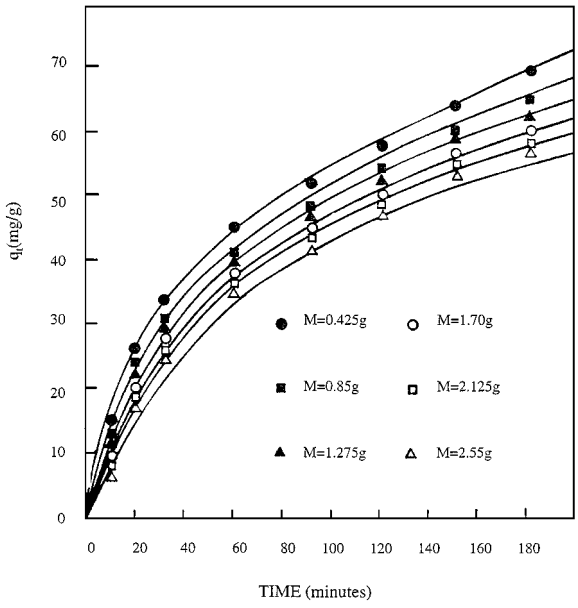

Figure 9. Effect of pith mass on the adsorption of BR22.

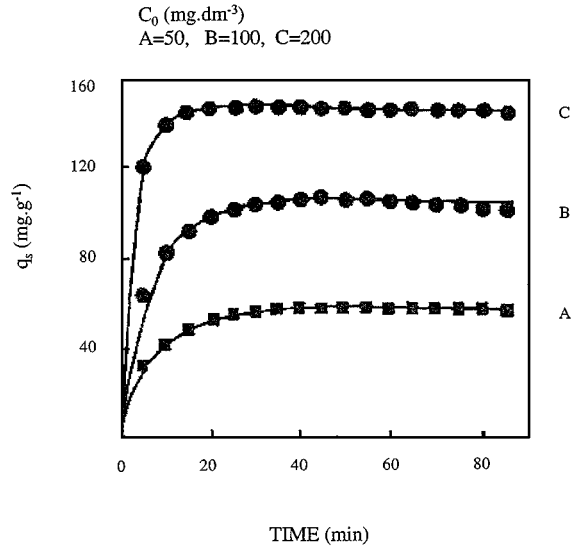

Figure 10. Solid phase concentration at particle surface q_s against contact time during the adsorption of BB69 onto pith.

surface area to dye mass ratio is not as high, since $C_0 = 200\ \text{mg} \cdot \text{dm}^{-3}$.

For high initial dye concentrations the surface concentrations, q_s and C_s, rise very rapidly and Figs. 10 and 11 show the variation of surface solid-phase concentration q_s and the liquid-phase concentration C_s at the surface of the particle for the adsorption of BB69 onto pith.

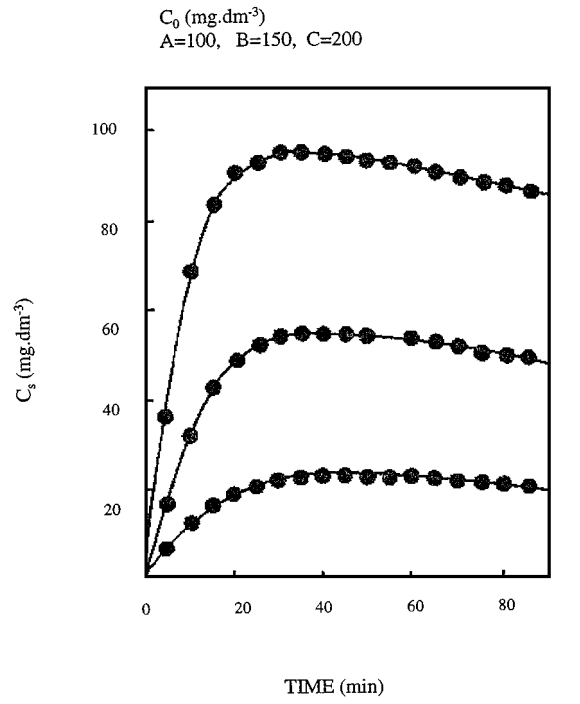

Figure 11. Liquid phase concentration at particle surface C_s against contact time during the adsorption of BB69 onto pith.

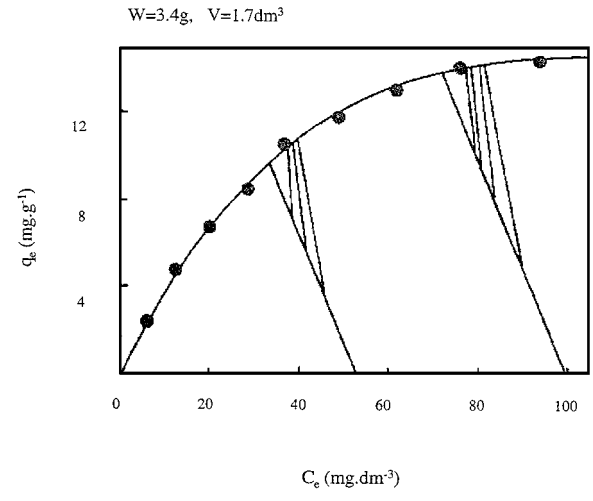

Figure 12. Equilibrium isotherm for AB25 onto pith showing operating lines and tie lines.

In Figs. 11 and 12 the bulk liquid concentration C_t decreases with time and it approaches the equilibrium curve along the operating line. The tie lines are drawn between the bulk liquid value of $(C_t, \bar{q}_t)$ and the surface equilibrium values (C_s, q_s). As time increases the tie lines move up the operating line and round

Table 5. External mass transfer and solid-phase diffusion coefficients for the adsorption of acid dyes onto pith.

Run No.	Dye	C_o (mg · dm^{-3})	M (g)	$k_f \times 10^{-5}$ (m s^{-1})	$D_s \times 10^{-12}$ (m^2 s^{-1})
1	BB69	50	1.7	2.0	1.1
2		100	1.7	2.0	1.1
3		150	1.7	2.0	1.1
4		200	1.7	2.0	1.1
5		250	1.7	2.0	1.1
6		300	1.7	2.0	1.1
7		200	0.425	2.0	1.1
8		200	0.85	2.0	1.1
9		200	1.275	2.0	1.1
10		200	1.70	2.0	1.1
11		200	2.125	2.0	1.1
12		200	2.55	2.0	1.1
1	BR22	50	1.7	1.5	1.0
2		100	1.7	1.5	1.0
3		150	1.7	1.5	1.0
4		200	1.7	1.5	1.0
5		250	1.7	1.5	1.0
6		300	1.7	1.5	1.0
7		200	0.425	1.5	1.0
8		200	0.85	1.5	1.0
9		200	1.275	1.5	1.0
10		200	1.70	1.5	1.0
11		200	2.125	1.5	1.0
12		200	2.55	1.5	1.0

$d_p = 605 \times 10^{-4}$ cm, agitation speed = 400 rpm, $T = 20^\circ$C, $V = 1.7$ dm^3 and $\rho_p = 0.804$ g · cm^{-3}.

the equilibrium curve. The solution of the problem involves calculating a surface liquid-phase equilibrium concentration C_s from the surface solid-phase concentration q_s.

The results for the effect of varying pith mass is shown in Tables 4 and 5 for a wide range of pith masses. The same values for the external mass transfer coefficients and the solid phase diffusion coefficients were obtained as in the initial dye concentration results. The correlation between experimental and theoretical results is again excellent except at high masses. At high masses there is low surface coverage and consequently the heterogeneity of the pith sites is probably important. This will result in D_s not being constant in certain cases, whereas for high loadings the effects of heterogeneous surface diffusion are swamped to a certain extent.

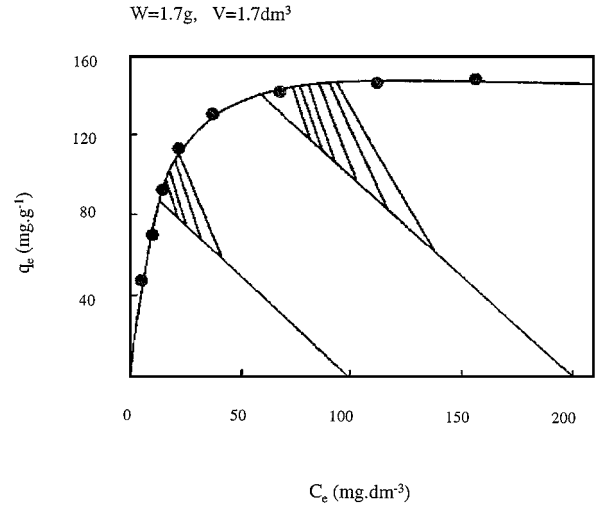

Figure 13. Equilibrium isotherm for BB69 onto pith showing operating lines and tie lines.

An alternative explanation is that the rate controlling step is dependent on both pore and surface diffusion whereby, the apparent diffusivity D_{eff} is given by (Fritz and Schlunder, 1981)

$$D_{\text{eff}} = \frac{D_{\text{mot}} \cdot \varepsilon_p}{\mu} + \rho_p \cdot D_s \frac{\partial q_e}{\partial C_e} \qquad (24)$$

where μ is the tortuosity factor.

From this equation it is apparent that the term $\partial q_e / \partial C_e$ will change rapidly with high masses which means operating lines terminating at low C_e values on the isotherms i.e., higher gradients for $\partial q_e / \partial C_e$.

The effective diffusion coefficient is based on a combination of a pore diffusion and a surface diffusion term and such a combined mechanism is possibly more applicable for high dye concentrations.

There are only limited data available in the literature reporting external mass transfer coefficients for the adsorption of dye ions. However, there are several papers in which external mass transfer coefficients, in well agitated batch adsorbers, have been determined for small organic molecules. These values, all using activated carbon, include values of 2.12×10^{-5}, 5.4×10^{-5}, 5.1×10^{-5} and 4.8×10^{-4} m s^{-1} for dodecyl benzene sulphonate, *p*-bromophenol, phenol and *p*-toluene sulphonate, respectively (Mathews and Weber, 1984); 2.0×10^{-5} and 1.0×10^{-5} m s^{-1} for AB25 and Basic Yellow 11, respectively (McKay, 1984a). Other values of 0.45×10^{-6} and 3.5×10^{-5} m s^{-1} were obtained by Allen (1981) for the

adsorption of AB25 ad BB69 onto peat, respectively. McKay (1984b) obtained a value of 2.0×10^{-6} m s^{-1} for the adsorption of BB69 onto silica. The values of external mass transfer coefficients obtained in this work are 8.0×10^{-6}, 5.0×10^{-6}, 2.0×10^{-5} and 1.5×10^{-5} m s^{-1} for the adsorption of AB25, AR114, BB69 and BR22 onto pith, respectively.

Hence, these values of external mass transfer coefficients are of a similar order of magnitude to those previously obtained by other workers for large organic molecules/ ions.

Values of solid phase diffusion coefficients have been given in the literature based on different initial solute concentrations and different adsorbent mass/-solution volume ratios. These include 1.58×10^{-12}, 2.0×10^{-12}, 0.99×10^{-13} and 1.38×10^{-12} m^2 s^{-1} for dodecyl benzene sulphonate, *p*-bromophenol, *p*-toluene sulphonate and phenol, respectively (Mathews and Weber, 1984); 2.0×10^{-13} and 3.0×10^{-14} m^2 s^{-1} for AB25 and Basic Yellow 11, respectively (McKay, 1984a). All the previous results were based on carbon adsorption. Other values of 1.5×10^{-13} and 2.1×10^{-13} m^2 s^{-1} were obtained by Allen (1981) for the adsorption of AB25 ad BB69 onto peat, respectively. McKay (1984b) obtained a value of 1.2×10^{-13} m^2 s^{-1} for the adsorption of BB69 onto silica. The values of solid phase diffusion coefficients obtained in this work are 6.0×10^{-13}, 3.0×10^{-13}, 1.1×10^{-12} and 1.0×10^{-12} m^2 s^{-1} for the adsorption of AB25, AR114, BB69 and BR22 onto pith, respectively.

The particular benefits of the solution to the model presented in this paper include the fact that there is no linear or pseudoirreversible restriction on the equilibrium isotherm. In addition, the main feature of the model is the semi-analytical solution linking dimensionless distance $z(r, R)$ with dimensionless time $\tau(D_s t/R^2)$ in all other solutions this relationship has to be solved by the more lengthy finite difference method.

Conclusion

Certain general points may be deduced from fitting the experimental and theoretical concentration time profiles:

1. Based on this HSD Model, a single external mass transfer coefficient and a single solid phase diffusion coefficient were obtained to predict concentration profiles for the variation of initial dye concentration and pith mass.
2. The model shows that the solid surface concentrations q_s and C_s rise very rapidly to the equilibrium values and then slowly decrease due to the inward diffusion of the adsorbate into the adsorbent pellet.
3. The HSDM can be used to describe experimental data with a high degree of accuracy up to three hours of contact time.
4. The model predictions are not so good for high adsorbent mass to dye mass ratios and for low adsorbent mass to dye mass ratios due to the fact that:

   - at high adsorbent mass to dye mass ratio surface heterogeneity or a varying D_s could affect the concentration decay curve;
   - at low adsorbent mass to dye mass ratios there is probably a contribution from pore diffusion.

Nomenclature

a_R	Redlich-Peterson isotherm constant	dm$^3\cdot$ mg^{-1}
A_p	Particle surface area	cm^2
C_o	Initial liquid-phase concentration	mg $\cdot$ dm^{-3}
C_s	Liquid-phase concentration at particle surface	mg $\cdot$ dm^{-3}
C_t	Liquid-phase concentration at time t	mg $\cdot$ dm^{-3}
d_p	Mean particle diameter	μm or cm
D_{eff}	Effective diffusion coefficient	cm$^2 \cdot$ s^{-1}
D_{mol}	Molecular diffusion coefficient	cm$^2 \cdot$ s^{-1}
D_s	Solid-phase diffusion coefficient	cm$^2 \cdot$ s^{-1}
j	Assignment of individual jth exponential term-equation	—
k_f	External mass transfer coefficient	cm $\cdot$ s^{-1}
K_R	Redlich-Peterson isotherm constant	dm$^3 \cdot$ g^{-1}
n	Number of experimental points	—
q	Solid-phase concentration	mg . g^{-1}
$\bar{q}_t$	Average solid-phase concentration in equilibrium with C_t	mg $\cdot$ g^{-1}
q_s	Solid-phase concentration at particle surface	mg $\cdot$ g^{-1}
r	Radial distance from the	cm

	centre of particle, $0 \leq r \leq R$	
R	Radius of adsorbent particle	cm or μm
t	Time	s, min or h
$u(z, \tau)$	Transformed solid-phase concentration in homogeneous solid-phase diffusion model ($= q(r/R)$)	—
V	Liquid-phase volume	dm^3
V_p	Volume of adsorbent particle	cm^3
W	Weight of adsorbent	g
z	Dimensionless radius ($= r/R$)	—
β	Redlich-Peterson isotherm constant	—
ε	Particle voidage	—
τ	Dimensionless time $[= (D_s \cdot t)/R^2]$	—
ρ_p	Density of particle	$g \cdot cm^{-3}$

References

Al Duri, B., *Reviews in Chemical Engineering*, **11**(2), 101 (1995).

Allen, S.J., Ph.D. Thesis, The Queen's University of Belfast, Northern Ireland, U.K, 1981.

Crittenden, J.C., Thesis, University of Michigan, 1976.

Crittenden, J.C. and W.J. Weber, Jr., *J. Env. Eng. Div. Amer. Soc. of Civil Engrs.*, **104**, 433 (1978a).

Crittenden, J.C. and W.J. Weber, Jr., *J. Env. Eng. Div. Amer. Soc. of Civil Engrs.*, **104**, 1175 (1978b).

Crittenden, J.C., P. Luft, D.W. Hand, J.L. Oravltz, S.W. Loper, and M. Arl, *Environ. Sci. Technol.*, **19**(11), 1037 (1985).

El-Dib, M.A., A.S. Moursy, and M.I. Badawy, *Water Research*, **12**, 1131 (1978).

Freundlich, H.Z., *J. Phys. Chem.*, **57**, 385 (1913).

Fritz, W. and E.U. Schlunder, *Chem. Eng. Sci.*, **36**, 721 (1981).

Glover, M.R.L., B.D. Young, and A.W. Bryson, *Internat. J. Mineral Processing*, **30**, 217 (1990).

Hashimoto, K., K. Miura, and S. Nagata *J. Chem. Eng. Japan*, **8**(5), 367 (1975).

Jossens, L., J.M. Prausnitz, W. Fritz, E.U. Schlunder, and A.L. Myers, *Chem. Eng. Sci.*, **33**, 1097 (1978).

Langmuir, I., *J. Amer. Chem. Soc.*, **40**, 2269 (1918).

Liapis, A.I. and D.W.T. Rippin, *Chem. Eng. Sci.*, **32**, 619 (1977).

Liapis, A.I. and D.W.T. Rippin, *Chem. Eng. Sci.*, **33**, 593 (1978).

Mathews, A.P., Thesis, University of Michigan (1975).

Mathews, A.P. and W.J. Weber, Jr., *AICHE. Symp. Ser.*, **73**(166), 91 (1976).

Mathews, A.P. and W.J. Weber, Jr., *Chem. Soc. Eng. Commun.*, **25**, 157 (1984).

McKay, G., *J. Chem. Tech. Biotechnol.*, **32**, 759 (1982).

McKay, G., *J. Chem. Tech. Biotechnol.*, **34A**, 294 (1984a).

McKay, G. and B. Al-Duri, *Chem. Eng. Sci.*, **43**(5), 1133 (1988).

McKay, G. and B. Al-Duri, *Chem. Eng. J.*, **41**, 9 (1989).

McKay, G. and B. Al-Duri, *J. Chem. Tech. Biotechnol.*, **48**, 269 (1990).

McKay, G. and S.J. Allen, *Can. J. Chem. Eng.*, **62**, 340 (1984b).

McKay, G., H.S. Blair, and J. Gardner, *J. Coll. Interf. Sci.* **95**(1), 108 (1983).

McKay, G., S. McKee, and H.R.J. Walters, *Chem. Eng. Sci.*, **42**(5), 1145 (1987).

McKay, G. and H.R.J. Walters, *Ind. Eng. Chem. Proc. Des. Dev.*, **23**, 181 (1984).

Miller, C.O. and C.W. Clump, *AICHE. J.*, **16**, 169 (1970).

Moon, H. and W.K. Lee, *J. Coll. Interf. Sci.*, **96**(1), 162 (1983).

Neretnieks, I., *Chem. Engng. Sci.*, **31**, 465 (1976).

Redlich, O.J. and D.L. Peterson, *J. Phys. Chem.* **63**, 1024 (1959).

Rice, R.G., *Chem. Eng. Sci.*, **37**, 83 (1982).

Saad, S.M., A.M. Nasser, M.T. Zimaity, and H.F. Abdel-Maged, *J. Oil Colour Chem. Ass.*, **61**, 43 (1978).

Seidel, A., G. Reschke, S. Friedrich, and D. Gelbin, *Ads. Sci. Technol.*, **3**, 189 (1986).

Smith, E.H., S. Tseng, and W.J. Weber, Jr., *Environ. Prog.*, **6**, 18 (1987).

Spahn, H. and E.U. Schlunder, *Chem. Eng. Sci.*, **30**, 529 (1975).

Thacker, W.E., J.C. Crittenden, and V.L. Snoeyink, *J. Water Poll. Control. Fed.*, **56**, 243 (1984).

Thomas, W.J. and J.L. Lombardi, *Trans. Inst. Chem. Engrs.*, **49**, 240 (1971).

Tien, C. *Can. J. Chem. Eng.*, 25 (1960).

Tien, C. *AICHE. J.*, **7**, 410 (1961).

Weber, W.J., Jr. and R.R. Rummer, *Water Resources Res.*, **1**, 361 (1965).

Young, B.D., J.D. Le Roux, and A.W. Bryson, *Hydrometallurgy*, **26**, 395 (1991).